Title: Protocerebral bridge neurons that regulate sleep in *Drosophila melanogaster*

Authors: Jun Tomita[1]*, Gosuke Ban[1]*, Yoshiaki S. Kato[1], and Kazuhiko Kume[1,2]

1. Department of Neuropharmacology, Graduate School of Pharmaceutical Sciences, Nagoya City University, Nagoya 467-8603, Japan

2. Corresponding author: Department of Neuropharmacology, Graduate School of Pharmaceutical Sciences, Nagoya City University, 3-1 Tanabe, Mizuho, Nagoya 467-8603, Japan.

Tel/Fax., +81-52-836-3676. Email, kume@phar.nagoya-cu.ac.jp

*These authors contributed equally to this work.

Acknowledgments: We thank Drs. Roland Strauss, Paul A. Garrity, Julie H. Simpson, Takaomi Sakai, J. Douglas Armstrong, Edward A. Kravitz and Barry J. Dickson, the Bloomington *Drosophila* Stock Center, the Vienna *Drosophila* RNAi Center and the Kyoto Stock Center for providing fly lines used in this study. In addition, we also thank Dr. Taro Ueno and members of the Kume lab for helpful discussions. This work was supported by Japan Society for the Promotion of Science (JSPS) KAKENHI Grant Numbers JP18H02481, K.K., JP26507008, JP17K08571, J.T.

Abstract

The central complex is one of the major brain regions that control sleep in *Drosophila*, but the circuitry details of sleep regulation have yet to be elucidated. We attempted to identify a novel sleep-regulating neuronal circuit in the central complex. *no-bridge*^{KS49} mutant flies with an anatomical defect in the protocerebral bridge (PB) significantly decreased sleep. By transient activation of a subset of the PB neurons using 14 *Gal4* drivers, we found the sleep-promoting *R59E08-Gal4* and the wake-promoting *R52B10-Gal4*. The *R59E08-Gal4* expressing PB neurons were identified as the PB interneurons according to their morphological features. On the other hand, using genetic mosaic analysis, we showed that activation of neurons projecting from the PB to the FB and contralateral NO (PFN neurons) in the *R52B10-Gal4* driver reduced sleep. A targeted GFP reconstitution across synaptic partners (t-GRASP) analysis demonstrated synaptic contacts between the sleep-promoting PB neurons and the wake-promoting PFN neurons. Furthermore, we found that activation of a pair of dopaminergic neurons with axons projecting the PB (T1 DA neurons) significantly decreased sleep. The wake-promoting T1 DA neurons were more likely to physically associate with the sleep-promoting PB interneurons. *Dopamine 2-like receptor* (*Dop2R*) knockdown in the *R59E08-Gal4* expressing PB interneurons significantly increased sleep. These results indicated that the neuronal circuit in the PB regulated by dopamine signaling mediates sleep-wakefulness.

Introduction

Sleep is a basic physiological state evolutionarily conserved among animal species (Allada and Siegel, 2008; Cirelli and Tononi, 2008). The fruit fly, *Drosophila melanogaster*, has emerged as a powerful model system for uncovering the molecular and cellular basis of sleep-wakefulness. Sleep in *Drosophila* is defined by behavioral features including circadian control of the timing of sleep, homeostasis of the amount of sleep and increased arousal threshold as in other animal species that do not exhibit the characteristic electroencephalogram patterns of sleep (Campbell and Tobler, 1984). The central complex is a unique midline neuropil structures in the adult insect brain, composed of four substructures, the protocerebral bridge (PB), the fan-shaped body (FB), the ellipsoid body (EB) and the noduli (NO), and serves as a higher-order integrator for sensory

62 information and various motor control (Homberg, 2008). Accumulating evidence from the
63 number of neurogenetic studies has established a crucial role for the central complex in
64 *Drosophila* sleep regulation. The sleep-promoting neurons having extensive presynaptic
65 arborizations in the dorsal layer of FB (dFB) has been identified (Donlea et al., 2011; Ueno et al.,
66 2012). Dopamine is a neurotransmitter that is essential for maintaining wakefulness in
67 *Drosophila*, similar to mammals (Andretic et al., 2005; Kume et al., 2005). The protocerebral
68 posterior medial 3 (PPM3) cluster dopamine neurons projecting to the dFB neurons controls sleep
69 through Dopamine 1-like receptor 1 (Dop1R1) signaling (Liu et al., 2012; Ueno et al., 2012).
70 Homeostatic mechanism of sleep would be associated with changes in neuronal activity of the
71 sleep-promoting dFB neurons and their functional upstream neurons, the R2 neurons in the EB
72 (Donlea et al., 2014; Liu et al., 2016). In addition, the dFB neurons form a recurrent circuit with
73 the EB R2 neurons via helicon cells to regulate sleep homeostasis (Donlea et al., 2018).
74 Regarding circadian regulation of sleep-wakefulness, recent studies have shown that sleep-
75 modulating dorsal neurons 1 (DN1) of circadian clock neurons and EB ring neuron subtypes are
76 functionally connected via sleep-promoting tubercular-bulbar (TuBu) neurons and that this circuit
77 is likely to regulate sleep-wakefulness (Guo et al., 2018; Lamaze et al., 2018). Besides, sleep-
78 promoting lateral posterior neurons (LPNs), another group of clock neurons, appear to form close
79 associations to the sleep-promoting dFB neurons and activate these neurons (Ni et al., 2019).
80 Detailed mechanisms for regulating sleep-wakefulness by the central complex are being clarified.
81 However, because the four substructures of the central complex are interconnected, a population
82 of central complex neurons other than the dFB neurons and EB R2 neurons should also be
83 implicated in the control of sleep-wakefulness. Here, we begin to explore a novel sleep-
84 regulating neuron in the central complex and discover that the sleep-promoting PB interneurons
85 have direct neuronal connections to the wake-promoting PB neurons projecting from the PB to
86 the FB and the NO. Moreover, we reveal that T1 cluster dopamine neurons regulate sleep by
87 acting on the sleep-promoting PB interneurons through D2 dopamine receptor signaling.
88

89 **Materials and Methods**

90 *Fly strains and rearing conditions*. Fruit flies (*Drosophila melanogaster*) were raised at 25ºC

91 in 50-60% relative humidity on standard medium containing cornmeal, yeast, glucose, wheat
92 germ and agar. They were maintained under a 12-h light:12-h dark (LD) cycle. Zeitgeber time
93 0 (ZT 0) corresponds to the light onset and ZT 12 to the light offset. Eleven mutant flies with
94 structural defects in the central complex *agnostic*^{X1} (*agn*^{X1}), *central-body-defect*^{KS171} (*cbd*^{KS171}),
95 *cbd*^{KS188}, *cbd*^{762}, *central-complex-broad*^{KS145} (*ccb*^{KS145}), *central-complex-deranged*^{KS135} (*ccd*^{KS135}),
96 *central-complex*^{KS181} (*cex*^{KS181}), *ellipsoid-body-open*^{KS263} (*ebo*^{KS263}), *ebo*^{678}, *ebo*^{1041} and *no-*
97 *bridge*^{KS49} (*nob*^{KS49}) were kindly provided by Roland Strauss. *UAS-dTrpA1* lines on the second
98 or third chromosomes were gifts from Paul A. Garrity. *tsh-Gal80*/CyO was a gift from Julie H.
99 Simpson. *Cha*$^{7.4kb}$*-Gal80* and *MB247-Gal80* were gifts from Takaomi Sakai. *c465-Gal4* was
100 a gift from J. Douglas Armstrong. *FLP*^{243} was a gift from Edward A. Kravitz.
101 *UAS>stop>mCD8::GFP* and *UAS>stop>dTrpA1* were gifts from Barry J. Dickson. *R14F09-*
102 *Gal4* (stock number: 48652), *R15E12-Gal4* (#48608), *R16D01-Gal4* (#48722), *R37G05-Gal4*
103 (#48133), *R38G07-Gal4* (#50019), *R40A01-Gal4* (#50072), *R44B10-Gal4* (#50202), *R45G06-*
104 *Gal4* (#50244), *R52B10-Gal4* (#38820), *R52G12-Gal4* (#49581), *R52H12-Gal4* (#38856),
105 *R55G08-Gal4* (#50422), *R59A12-Gal4* (#39206), *R59E08-Gal4* (#39219), *R67B06-Gal4*
106 (#48294), *R74C08-Gal4* (#46711) *R83A10-Gal4* (#48371), *R83H12-Gal4* (#40374), *R91A12-*
107 *Gal4* (#40573), *10×UAS-IVS-mCD8::GFP* (#32187), *10×UAS-IVS-mCD8::GFP* (#32188),
108 *UAS-DenMark*, *UAS-syt.eGFP* (#33064), *R52B10-LexA* (#52826), *R59E08-LexA* (#52832),
109 *13×LexAop2-post-t-GRASP*, *20×UAS-pre-t-GRASP* (#79040), *UAS-CD4-spGFP1-10*, *lexAop-*
110 *CD4-spGFP11* (#58755), *UAS-Dop2R-RNAi* (#50621) and *y*, *v*; *P{CaryP}attP40* (control line for
111 TRiP RNAi lines, #36304) were obtained from the Bloomington *Drosophila* Stock Center,
112 Indiana University, Indiana, USA. *UAS-Dop2R-RNAi* (VDRC ID: 1820), *UAS-Dicer-2* (60008)
113 and *w*^{1118} (the genetic background for VDRC RNAi lines, 60000) were from the Vienna
114 *Drosophila* RNAi Center (VDRC). *P{neoFRT}19A* (stock number: 106482) and
115 *P{neoFRT}19A*, *tubP-GAL80*, *hsFLP*; *Pin*^{Yt}/CyO (#108064) were from the Kyoto Stock Center,
116 Kyoto Institute of Technology, Kyoto, Japan.
117
118 *Locomotor activity and sleep analysis*. Locomotor activity of individual fly was measured using
119 the *Drosophila* activity monitoring system (TriKinetics) as described previously. Flies were
120 placed individually in glass tubes (length, 65 mm; inside diameter, 3 mm) containing either
121 standard medium or sucrose-agar medium (5% sucrose and 1% agar) at one end and were
122 entrained for at least 3 days to LD cycles before transferring to constant dark (DD) conditions.

123 Two- to four-day-old male flies were used except for MARCM experiments. Activity data were
124 recorded continuously at 1-min intervals under both LD and DD conditions. *Drosophila* sleep
125 was defined as continuous immobile periods lasting 5 min or longer based on previous reports
126 (Hendricks et al., 2000; Shaw et al., 2000; Huber et al., 2004; Kume et al., 2005). Total activity
127 counts, total amount of sleep and waking activity index were analyzed by Microsoft Excel-based
128 software as previously described and averaged over 3 days. For conditional dTrpA1 activation
129 experiments, control and experimental flies were grown at 22ºC. Sleep measurements were
130 performed in DD following LD cycles. The temperature was raised from 22ºC to 29ºC for 24 h
131 or 48 h to activate dTrpA1-expressing neurons and then returned to 22ºC.
132
133 *Video tracking of locomotion*. Offspring from the control (*R59E08-Gal4* × *tsh-Gal80*) and the
134 experimental (*R59E08-Gal4* × *tsh-Gal80*; *UAS-dTrpA1*) crosses were housed in glass tubes and
135 entrained to an LD cycle at 22ºC. After entrainment, these flies were maintained in DD with
136 illumination by near-infrared LEDs. At circadian time (CT) 0 on day 2 in DD, flies were
137 transferred from 22ºC to 29ºC for 12 h to activate dTrpA1. The behavior of flies was recorded
138 at 2 frames/sec using a USB camera (Flea3 USB3.0: FL3-U3-13Y3M-C, Point Grey Research
139 Inc.) during late subjective day (CT 8 to CT 12) at 29ºC. The captured images were converted
140 into 8-bit grayscale images. A composite background image was subtracted from each video
141 image. The position of the center of mass for individual fly was calculated for each subtracted
142 image using the Particle Tracker 2D/3D, an ImageJ plugin (Sbalzarini and Koumoutsakos, 2005).
143
144 *The MARCM system*. To generate flies for MARCM, female flies carrying *FRT19A*, *tub-GAL80*,
145 *hs-FLP*; *UAS-dTrpA1* (X ; II) crossed to males carrying *FRT19A*; *R52B10-Gal4*, *10×UAS-IVS-*
146 *mCD8::GFP* (X ; III) at 22ºC. Following egg-laying for 48 h, embryos or first instar larvae were
147 heat-shocked at 37ºC for 1 h to induce FLP-mediated recombination across two FRT sites. The
148 amount of sleep in mosaic female flies was measured at 22ºC and 29ºC under DD conditions.
149 After sleep analysis, GFP expression co-expressed with dTrpA1 in the brains was
150 immunohistochemically determined.
151
152 *Immunohistochemistry*. To detect GFP expression in the MARCM experiments and
153 reconstituted GFP signals in the t-GRASP and GRASP experiments, whole-mount
154 immunofluorescence staining of adult brains was performed as described (Wu and Luo, 2006).

155 For determination of GFP expression, GFP polyclonal antibody (A6455, Invitrogen) was used at
156 1:250 dilution and goat anti-rabbit IgG, Alexa Fluor 568 (A11036, Invitrogen) was used at 1:200
157 dilution as secondary antibodies. We used GFP recombinant rabbit monoclonal antibody
158 (G10362, Invitrogen) at 1:300 dilution and monoclonal anti-GFP, clone GFP-20 (G6539, Sigma-
159 Aldrich) at 1:100 dilution for detection of reconstituted GFP signals in t-GRASP and GRASP
160 experiments, respectively. Alexa Fluor 488, goat anti-rabbit IgG (A11008, Invitrogen) and goat
161 anti-mouse IgG (A11001, Invitrogen) were used at 1:200 dilution as secondary antibodies.
162 Immunostained brain tissues were imaged by laser scanning confocal microscopes Zeiss LSM
163 510 or LSM 800 (Carl Zeiss). Adult brains and ventral nerve cords expressing *mCD8::GFP* or
164 *syt-GFP* under the control of Gal4 were dissected and scanned by the confocal microscopes
165 without staining.
166
167 *Statistical analysis*. Data were analyzed as described in the figure legends using Microsoft
168 Excel and R: a language and environment for statistical computing (R Core Team, 2020,
169 https://www.R-project.org/).
170
171 **Results**
172 **The PB defective mutant flies, *nob*^{KS49} decreased sleep**
173 In order to examine the role of the CC in sleep regulation, we tested eleven mutant strains with
174 morphological defects in the CC. These mutant flies were isolated histologically following ethyl
175 methanesulfonate mutagenesis, except for *agn*^{X1}, which was isolated from a wild population
176 (Strauss and Heisenberg, 1993). Flies were entrained to 12 h light : 12 h dark (LD) cycles for at
177 least 3 days, then maintained in constant dark (DD) conditions. Locomotor activity was
178 recorded in both LD and DD conditions. Sleep was defined as periods of immobile state lasting
179 5 min or longer, as previously described (Hendricks et al., 2000; Shaw et al., 2000; Huber et al.,
180 2004; Kume et al., 2005). Because most of these CC structural mutants are still uncharacterized,
181 their total daily activity and sleep were compared to those of three control strains (Canton-S (CS),
182 *y w* and *w*^{1118}) under constant dark (DD) conditions. There were no significant differences in
183 total daily activity and sleep between the three control strains (*Figure 1A,B*). Among the CC
184 mutant strains tested, *nob*^{KS49} flies showed significant hyperactivity compared with two control
185 lines (CS and *y w*). *nob*^{KS49} mutants have a defect in the central part of PB (Strauss et al., 1992).
186 No difference was seen in waking activity index, defined as total daily activity divided by the

active period length, between *nob*^{KS49} and controls, suggesting hyperactivity in *nob*^{KS49} flies is not attributed to aberrant locomotion (*Figure 1C*). On average, total daily activity significantly increased by about 2-fold in *nob*^{KS49} relative to controls (*Figure 1A*). In contrast, total daily sleep of *nob*^{KS49} flies decreased to approximately half of that of the CS and *y w* controls (*Figure 1B*). These results suggest that PB is involved in sleep regulation.

Activation of *Gal4*-expressing neurons in *Gal4* drivers that express in the PB affected sleep

To further explore the involvement of PB neurons in sleep regulation, we examined the effects of transient thermogenetic activation of a subset of PB neurons using the temperature-sensitive cation channel dTrpA1 on the amount of sleep. For this, fourteen *Gal4* driver lines that express strongly in PB neurons (*PB-Gal4*) were selected from the Gal4 image data of the FlyLight Image Database (https://flweb.janelia.org/cgi-bin/flew.cgi; Jenet t et al., 2012). Progenies from the control (*PB-Gal4* × *w*^{1118}) and the experimental (*PB-Gal4* × *UAS-dTrpA1*) crosses were grown at 22ºC to adulthood. Sleep was measured in adult progeny flies in DD following LD cycles. These flies were transferred from 22ºC to 29ºC for 24 h to conditionally activate dTrpA1-expressing neurons and then returned to 22ºC. Of the 14 *PB-Gal4* drivers tested, the acute activation of neurons with the 9 *Gal4* drivers significantly decreased sleep. In particular, the decrease in the sleep amount induced by activation of neurons using the *R52B10-Gal4* was most remarkable and flies hardly slept during neuronal activation as previously reported (*Figure 2A,B*) (Liu et al., 2016). Although clear homeostatic sleep recovery (sleep rebound) after sleep loss by the thermogenetic activation using the *R52B10-Gal4* was reported (Liu et al., 2016), such a clear sleep rebound was not observed in our experimental conditions (*Figure 2B*). On the other hand, the activation of Gal4 expressing neurons in the 3 of 14 *PB-Gal4* drivers significantly increased sleep (*Figure 2A*). The largest effect on sleep induction was caused by the neuronal activation using the *R59E08-Gal4*. In this *Gal4* driver, the amount of sleep in the experimental flies peaked in the middle of the subjective day at 29ºC as much as the control flies and was maintained at the peak level during neuronal activation (*Figure 2C*). Sleep amount in the experimental flies was significantly reduced compared with that in the control flies for at least 2 days after stopping the activation. The expression patterns of the *R52B10-Gal4* or the *R59E08-Gal4* drivers in the adult brains were visualized using *UAS-mCD8::GFP*. The wake-promoting *R52B10-Gal4* drove strong expression in several cell types of neurons named PFN projecting from the PB to the ventral part of the FB and contralateral NO (*Figure 2D*) as shown in the FlyLight and the previous

219 report (Buchanan et al., 2015). In addition to these central complex substructures, some neurons
220 in the anterior ventrolateral protocerebrum (AVLP) were also be seen as intense GFP signals
221 (*Figure 2D*). The thermogenetic activation using the *R52H12-Gal4* or the *R83A10-Gal4* that
222 express strongly in the AVLP neuropil did not result in a marked decrease in the amount of sleep
223 (FlyLight and *Figure 2-figure supplement 1*). The sleep-promoting *R59E08-Gal4* specifically
224 labeled the PB strongly in the central complex (*Figure 2E*). These PB neurons were identified
225 as PB interneurons according to their previously described morphological features (Lin et al.,
226 2013; Wolff et al., 2015). In addition, the ubiquitous strong expression of GFP in the medulla
227 cells was also detected in the *R59E08-Gal4* driver. Neuronal activation using two *Gal4* drivers
228 (*R14F09-Gal4* and *R59A12-Gal4*), whose expression patterns in the medulla resemble that of the
229 *R59E08-Gal4*, did not significantly increase the amount of sleep (FlyLight and *Figure 2-figure*
230 *supplement 2*).
231
232 **Activation of PB interneurons with *R59E08-Gal4* increased sleep**
233 The sleep-promoting *R59E08-Gal4* was expressed not only in the adult brain but also in the
234 ventral nerve cord (VNC) (*Figure 3A*). To determine which targeted neurons in this driver are
235 responsible for the sleep induction, we employed *tsh-Gal80*, which inhibits Gal4-mediated
236 transcription in the VNC. The incorporation of the *tsh-Gal80* transgene successfully blocked
237 *R59E08-Gal4* induced GFP expression in the VNC without affecting its expression pattern in the
238 brain (*Figure 3A*). Activation of *R59E08-Gal4*-expressing neurons with *tsh-Gal80* also
239 markedly increased in the amount of sleep, indicating that brain neurons labeled by *R59E08-Gal4*
240 contribute dTrpA1-mediated sleep induction (*Figure 2B* and *Figure 3A*). On the other hand,
241 decreased sleep caused after dTrpA1 activation was completely restored by introducing *tsh-Gal80*,
242 indicating that *R59E08-Gal4*-expressing the VNC neurons are involved in this sleep phenotype.
243 Thus, distinct populations of *R59E08-Gal4*-expressing neurons participate in the sleep
244 phenotypes induced during or after dTrpA1 activation. Because the DAM system only detects
245 motions of a fly passing through an infrared beam that bisects a glass tube at the center, continuing
246 feeding or grooming away from the beam path are detected as apparent inactivity (continuous
247 bins with the value of zero). To confirm that the flies certainly sleep by activation of *R59E08-*
248 *Gal4*-expressing brain neurons, we performed video analysis of the behavior of these flies in glass
249 tubes during the late subjective-day (CT 8 to CT 12) at 29ºC (*Figure 3C*). The temperature was
250 shifted from 22ºC to 29ºC at CT 0. As expected from the sleep patterns observed by the DAM

251 system, the experimental flies (*R59E08-Gal4* × *tsh-Gal80*; *UAS-dTrpA1*) displayed little
252 locomotor activity compared to controls (*R59E08-Gal4* × *tsh-Gal80*). The immobile flies did
253 not show excessive feeding or grooming, and paralysis in naked-eye observation. We also found
254 that the sleep phenotypes induced during or after activation of *R59E08-Gal4*-expressing neurons
255 were fully rescued by introducing $Cha^{7.4kb}$-*Gal80* transgene, which prohibits Gal4 activity in
256 cholinergic neurons (*Figure 3D*). Taken together, these results indicate that the sleep-promoting
257 PB interneurons were cholinergic.
258
259 **PFN neurons were wake-promoting neurons**
260 As shown in *Figure 4A*, *tsh-Gal80* effectively attenuated the wake-promoting *R52B10-Gal4*
261 driven GFP expression in the VNC without effect on its expression in the brain. Activation of
262 the brain neurons targeted by *R52B10-Gal4* resulted in a dramatic reduction in the amount of
263 sleep comparable to that evoked by activating both the brain and the VNC neurons using this
264 *Gal4* driver (*Figure 2C* and *Figure 4B*). Next, we searched for *R52B10-Gal4*-expressing brain
265 neurons that contribute to the promotion of wakefulness by genetic mosaic approach. Using the
266 mosaic analysis with a repressible cell marker (MARCM) system, the *dTrpA1* and *GFP* were
267 randomly co-expressed in a subpopulation of neurons using *R52B10-Gal4* with FRT/FLP-induced
268 mitotic recombination. We measured the amount of sleep in these genetically mosaic flies at
269 22ºC and then 29ºC under DD conditions. The change in sleep amount (ΔSleep) in individual
270 flies was calculated by subtracting the amount of sleep during the 12-h subjective night at 29ºC
271 from that at 22ºC (*Figure 4C*). In this experiment, ΔSleep value above the mean plus two times
272 standard deviation (+2 SD) was regarded as a significant decrease in subjective-night sleep at
273 29ºC. Of 133 flies examined, 7 flies had a ΔSleep value above the mean +2 SD (426 min).
274 After measuring the amount of sleep, the brains of these flies were dissected and immunostained
275 to determine GFP expression co-expressed with dTrpA1. GFP expression in the flies with
276 significantly reduced sleep labeled the PFN neurons in all but one of the flies shown in #7 in
277 *Figure 4D*. By contrast, in the 7 individuals having ΔSleep value near the average, 2 flies were
278 labeled with the PFN neurons (#5 and #6 in *Figure 4E*), while the remaining flies were either not
279 labeled at all (#1 and #2) or labeled with neurons different from the PFN neurons (#3, #4, #7).
280 Moreover, to ensure that the PFN neurons labeled by *R52B10-Gal4* are the wake-promoting
281 neurons, we employed *c465-Gal4* that drives expression in these neurons participating in the
282 tuning of the magnitude of locomotor handedness (Buchanan et al., 2015). Because *c465-Gal4*

283 is also strongly expressed in the mushroom bodies that is another brain neuropil structures
284 involved in *Drosophila* sleep regulation (Joiner et al., 2006; Pitman et al., 2006; Sitaraman et al.,
285 2015a), we used *MB247-Gal80*, which blocks the activity of Gal4 in the mushroom bodies
286 (*Figure 4F*). As expected, activation of *c465-Gal4*-expressing neurons except for mushroom
287 body neurons significantly decreased sleep, as did the activation of *R52B10-Gal4*-expressing
288 neurons (*Figure 4G*). These results indicate that the PFN neurons labeled by *R52B10-Gal4* are
289 wake-promoting.
290
291 **PFN neurons had synaptic connections with the sleep-promoting PB interneurons**
292 To visualize putative dendritic and axonal terminals of the wake-promoting PFN neurons, both
293 DenMark, a specific somatodendritic marker and synaptotagmin (syt)-GFP, a presynaptic marker
294 localized to synaptic vesicles were expressed using *R52B10-Gal4*. These neurons displayed
295 specific dendritic DenMark labeling in the PB and strong labeling of presynaptic syt-GFP in the
296 layer 1 of the FB and in the ventral NO (*Figure 5A*). In addition, weak labeling of presynaptic
297 terminals was also observed near the layers 2 to 3 of the FB and in regions of the NO other than
298 the ventral NO. To assess synaptic connectivity between the sleep-promoting PB interneurons
299 and the wake-promoting PFN neurons, we employed a targeted GFP reconstitution across
300 synaptic partners (t-GRASP) technique (Shearin et al., 2018) under the control of two independent
301 binary systems. A part of the *cacophony* gene tagged with the *GFP11* fragment of a *split-GFP*
302 (*pre-t-GRASP*), which is targeted to axonal terminals and a portion of the mouse *Icam5* gene
303 tagged with the *GFP1-10* (*post-t-GRASP*), which is targeted to dendritic terminals were expressed
304 by *R59E08-Gal4* and *R52B10-LexA*, respectively. Reconstituted GFP signals were detected in
305 the PB (*Figure 5B*), suggesting that the sleep-promoting PB interneurons labeled by *R59E08-*
306 *Gal4* have synaptic connections with the wake-promoting PFN neurons marked by *R52B10-Gal4*.
307
308 **Dopamine signaling acted on the sleep-promoting PB interneurons for sleep regulation**
309 Dopamine has been identified as a key neurotransmitter in the regulation of sleep in *Drosophila*
310 (Andretic et al., 2005; Kume et al., 2005; Pimentel et al., 2016). In the *Drosophila* brain,
311 dopaminergic (DA) neurons are distributed in clusters, and each cluster is involved in various
312 physiological phenomena, including sleep-wake (Liu et al., 2012; Ueno et al., 2012; Sitaraman et
313 al., 2015b). A pair of DA neurons, named T1, has been previously observed with dendrites
314 arborizing in the tritocerebrum and with axons projecting to the PB (Nässel and Elekes, 1992;

315 Alekseyenko et al., 2013). The intersectional method combining the enhancer-trap flippase
316 (FLP) transgenic line, *FLP*^{243} with a DA-neuron specific *TH-Gal4* driver allows for the selective
317 targeting of the T1 neurons (*Figure 6A*) (Alekseyenko et al., 2013). Both activation and
318 inhibition of the T1 DA neurons using this intersectional method have been reported to
319 specifically facilitate inter-male aggression. On the other hand, inactivation of these neurons
320 has no effect on locomotor activity and sleep amount (Alekseyenko et al., 2013). We
321 conditionally activated the T1 neurons with dTrpA1 and found that the manipulation resulted in
322 a significant decrease in the amount of sleep (*Figure 6B*). Next, we examined whether T1 DA
323 neurons directly connect with sleep-wake regulating PB neurons by GRASP analysis utilizing
324 membrane-tethered two complementary split-GFP fragments (CD4-spGFP1-10 and CD4-
325 spGFP11) (Feinberg et al., 2008). *TH-Gal4* was used to express *UAS-CD4-spGFP1-10* and
326 *R59E08-LexA* or *R52B10-lexA* were employed to drive *lexAop-CD4-spGFP11*, respectively.
327 Immunohistochemical signals for reconstituted GFP in the PB were detected only in the
328 combination of *TH-Gal4* and *R59E08-LexA* (*Figure 6C,D*). These signals were dot-like and
329 localized to the bilateral bends of the PB. Alekseyenko and colleagues also demonstrate that
330 Dopamine 2-like receptors (Dop2R also known as D2R or DD2R), a functional counterpart of
331 mammalian D2 receptor, are expressed in the PB but not localized to the presynaptic terminals of
332 T1 neurons. *Dop2R* knockdown using two independent RNAi lines in the *R59E08-Gal4*
333 expressing PB neurons resulted in a significant increase in the amount of sleep compared to
334 controls (*Figure 6E* and *Figure 6-figure supplement 1*). These results support the idea that T1
335 DA neurons regulate sleep by acting on the sleep-promoting PB interneurons via D2 receptor
336 signaling.
337
338 **Discussion**
339 The data presented provide evidence that *Drosophila* sleep is controlled by the neuronal circuit
340 in PB consisting of the wake-promoting PFN neurons and the sleep-promoting PB interneurons
341 and by the T1-PB dopamine pathway. Previous anatomical, electrophysiological and genetic
342 studies have revealed the physiological functions of the PB in several insect species. For
343 example, in desert locusts, different types of the PB neurons generate a topographical map of the
344 sky polarization pattern underlying sun compass orientation (Homberg et al., 2011).
345 Morphological counterparts of these locust's PB neurons are found in migratory monarch
346 butterflies and serve similar functions in processing polarized-light information (Heinze and

347 Reppert, 2011). Experiments in fruit flies have demonstrated a role for the PB in locomotor
348 control such as walking speed, leg coordination, maintenance of walking activity, locomotor
349 handedness and visual targeting in gap-crossing behavior (Strauss et al., 1992; Strauss and
350 Heisenberg, 1993; Martin et al., 1999; Triphan et al., 2010; Buchanan et al., 2015). The
351 locomotor activity of *nob*^{KS49} mutants has been reported to be decreased compared to control flies
352 but was increased in the present study (Martin et al., 1999) (*Figure 1A*). We and Martin et al.
353 assessed the number of activity counts per day or at a particular time of day (4.5 hours) in *nob*^{KS49}
354 flies as total locomotor activity, respectively. This difference in assessment methods may have
355 caused the phenotypic discrepancy in locomotor activity. *nob*^{KS49} flies with a large gap at the
356 sagittal midplane in the PB showed a significant reduction in the amount of sleep (*Figure 1B*),
357 suggesting a physical impairment of sleep-promoting neurons in this mutant. We found that
358 *R59E08-Gal4*-expressing PB interneurons promote sleep (*Figure 2* and *Figure 3*). Analysis of
359 single PB neurons labeled by MARCM or multicolor flip-out technique has shown that PB
360 interneurons are classified into three cell types based on their pattern of glomerular innervation
361 in the PB (Lin et al., 2013; Wolff et al., 2015). Two of the three cell types of PB interneurons
362 innervate all glomeruli, including the central part of the PB. Because the sleep-promoting
363 *R59E08-Gal4* was expressed throughout the PB, at least one of these two cell types of PB
364 interneurons would have been labeled with this driver. Although the cell type of PB interneurons
365 that promote sleep has been unidentified in our results, the two cell types may be physically
366 damaged in *nob*^{KS49} mutants.
367 Our MARCM experiment using *R52B10-Gal4* suggested that distinct types of PFN neurons
368 promote wakefulness (*Figure 2C,E*). There are five cell types of PFN neurons, which are PB
369 output neurons, classified according to their patterns of projection to FB and NO (Wolff et al.,
370 2015). Each PFN neuron belonging to each cell type arborizes in one PB glomerulus and
371 projects to one FB layer and to one contralateral NO. The *Gal4* line *c465* drives expression in
372 the wake-promoting PFN neurons (*Figure 4F,G*) (Lin et al., 2013; Buchanan et al., 2015). Of
373 the five cell types of PFN neurons, three are commonly labeled by *R52B10-Gal4* and *c465-Gal4*,
374 especially the cell type with axon terminals in layer 2 of the FB and in the ventral NO exhibits
375 high *Gal4* expression in these two drivers (Buchanan et al., 2015). On the other hand, neuronal
376 activation with *R44B10-Gal4*, which high expression in all three cell types of PFN neurons
377 (Buchanan et al., 2015), was less effective in reducing the amount of sleep than neuronal
378 activation with *R52B10-Gal4* or *c465-Gal4* (*Figure 2A*). Although *R52B10-Gal4*, *c465-Gal4*

379 and *R44B10-Gal4* label the same cell types of PFN neurons, it is possible that PFN neurons
380 arborizing in one specific PB glomerulus are implicated in promoting arousal and that these
381 neurons are co-labeled with *R52B10-Gal4* and *c465-Gal4*.
382 The t-GRASP experiment using *R59E08-Gal4* and *R52B10-LexA* suggested the sleep-promoting
383 PB interneurons form synaptic contacts with the wake-promoting PFN neurons (*Figure 5B*).
384 The symmetrical patterns of the t-GRASP signal intensity in PB glomeruli should indicate that
385 this signal is not non-specific, supporting the idea described above that particular subtypes of
386 PFN neurons promote arousal. Sleep phenotypes of the flies in which *R59E08-Gal4*- or
387 *R52B10-Gal4*-expressing neurons were acutely activated, and axon-dendrite connectivity
388 between these sleep-regulating neurons suggest that the sleep-promoting PB interneurons inhibit
389 the activity of the wake-promoting PFN neurons. Because the sleep-promoting PB
390 interneurons were cholinergic (*Figure 3D*), the wake-promoting PFN neurons were likely to be
391 regulated by inhibitory acetylcholine receptor signaling (Ren et al., 2015). Functional
392 connectivity analysis of the central complex using Ca^{2+} imaging combined with optogenetics
393 has demonstrated that activation of one cell type of PB interneurons designated as Δ7 triggers
394 the inhibitory response of one cell type of PFN neurons (Franconville et al., 2018). However,
395 since the Δ7 neurons are either glutamatergic or GABAergic, they must not be the sleep-
396 promoting PB interneurons. Further anatomical and functional dissection of the sleep-
397 regulating neuronal circuits in the PB archived with promising *split-Gal4* lines will be required.
398 Previous studies have elucidated the control of *Drosophila* sleep by several clusters of DA
399 neurons (Liu et al., 2012; Ueno et al., 2012; Sitaraman et al., 2015b). This study revealed that
400 the PB-projecting T1 DA neurons physically connected to the sleep-promoting PB interneurons
401 promote wakefulness (*Figure 6A-D*). Because knockdown of *Dop2R* encoding Gi protein-
402 coupled dopamine receptor in *R59E08-Gal4*-expressing neurons significantly increased the
403 amount of sleep (*Figure 6E* and *Figure 6-figure supplement 1*), the simplest explanation is that
404 dopamine inhibits the sleep-promoting PB interneurons and thus promotes wakefulness. *Dop2R*
405 null mutants have an increased amount of sleep (Deng et al., 2019). The DopR2 function in the
406 pars intercerebralis (PI) neurons expressing Dilp2 and SIFamide has been shown to contribute to
407 this sleep-increasing phenotype. Our results show that, in addition to the PI, Dop2R also
408 functions in the PB to regulate sleep. T1 neurons were originally identified as neurons that
409 specifically modulate aggression between pairs of males (Alekseyenko et al., 2013). Regarding
410 the interaction between sleep and aggression, it has been shown that aggressive behaviors are

411 suppressed in sleep-deprived male flies, and the changes are mediated by octopamine signaling
412 (Kayser et al., 2015). Elucidation of the mechanisms controlling the activity of T1 neurons may
413 provide a novel link between sleep and aggression.
414 More recently, we have successfully demonstrated that the wake-promoting PFN neurons
415 directly activate the FB interneurons (also known as pontine neurons) that appear to transmit
416 inhibitory acetylcholine signals to the sleep-promoting dFB neurons (Kato YS et al., unpublished
417 results). Further studies are required to determine the cellular and molecular details of how these
418 PB-dFB circuits control sleep-wakefulness.
419
420 **References**

421 Alekseyenko, O. V., Chan, Y.-B., Li, R., and Kravitz, E. A. (2013). Single dopaminergic
422 neurons that modulate aggression in Drosophila. *Proc. Natl. Acad. Sci. U. S. A.* 110, 6151–
423 6. doi:10.1073/pnas.1303446110.
424 Allada, R., and Siegel, J. M. (2008). Unearthing the phylogenetic roots of sleep. *Curr. Biol.* 18,
425 R670–R679. doi:10.1016/j.cub.2008.06.033.
426 Andretic, R., van Swinderen, B., and Greenspan, R. J. (2005). Dopaminergic modulation of
427 arousal in Drosophila. *Curr. Biol.* 15, 1165–75. doi:10.1016/j.cub.2005.05.025.
428 Buchanan, S. M., Kain, J. S., and de Bivort, B. L. (2015). Neuronal control of locomotor
429 handedness in Drosophila. *Proc. Natl. Acad. Sci.* 112, 6700–6705.
430 doi:10.1073/pnas.1500804112.
431 Campbell, S. S., and Tobler, I. (1984). Animal sleep: a review of sleep duration across
432 phylogeny. *Neurosci. Biobehav. Rev.* 8, 269–300. doi:10.1016/0149-7634(84)90054-x.
433 Cirelli, C., and Tononi, G. (2008). Is sleep essential? *PLoS Biol.* 6, e216.
434 doi:10.1371/journal.pbio.0060216.
435 Deng, B., Li, Q., Liu, X., Cao, Y., Li, B., Qian, Y., et al. (2019). Chemoconnectomics: Mapping
436 Chemical Transmission in Drosophila. *Neuron* 101, 876-893.e4.
437 doi:10.1016/j.neuron.2019.01.045.
438 Donlea, J. M., Pimentel, D., and Miesenböck, G. (2014). Neuronal machinery of sleep
439 homeostasis in Drosophila. *Neuron* 81, 860–72. doi:10.1016/j.neuron.2013.12.013.
440 Donlea, J. M., Pimentel, D., Talbot, C. B., Kempf, A., Omoto, J. J., Hartenstein, V., et al.
441 (2018). Recurrent Circuitry for Balancing Sleep Need and Sleep. *Neuron* 97, 378-389.e4.
442 doi:10.1016/j.neuron.2017.12.016.

443 Donlea, J. M., Thimgan, M. S., Suzuki, Y., Gottschalk, L., and Shaw, P. J. (2011). Inducing
444 sleep by remote control facilitates memory consolidation in Drosophila. *Science* 332,
445 1571–6. doi:10.1126/science.1202249.
446 Feinberg, E. H., Vanhoven, M. K., Bendesky, A., Wang, G., Fetter, R. D., Shen, K., et al.
447 (2008). GFP Reconstitution Across Synaptic Partners (GRASP) defines cell contacts and
448 synapses in living nervous systems. *Neuron* 57, 353–63.
449 doi:10.1016/j.neuron.2007.11.030.
450 Franconville, R., Beron, C., and Jayaraman, V. (2018). Building a functional connectome of the
451 drosophila central complex. *Elife*. doi:10.7554/eLife.37017.
452 Guo, F., Holla, M., Díaz, M. M., and Rosbash, M. (2018). A Circadian Output Circuit Controls
453 Sleep-Wake Arousal in Drosophila. *Neuron* 100, 624-635.e4.
454 doi:10.1016/j.neuron.2018.09.002.
455 Heinze, S., and Reppert, S. M. (2011). Sun compass integration of skylight cues in migratory
456 monarch butterflies. *Neuron* 69, 345–58. doi:10.1016/j.neuron.2010.12.025.
457 Hendricks, J. C., Finn, S. M., Panckeri, K. A., Chavkin, J., Williams, J. A., Sehgal, A., et al.
458 (2000). Rest in Drosophila is a sleep-like state. *Neuron* 25, 129–38. doi:10.1016/s0896-
459 6273(00)80877-6.
460 Homberg, U. (2008). Evolution of the central complex in the arthropod brain with respect to the
461 visual system. *Arthropod Struct. Dev.* 37, 347–62. doi:10.1016/j.asd.2008.01.008.
462 Homberg, U., Heinze, S., Pfeiffer, K., Kinoshita, M., and el Jundi, B. (2011). Central neural
463 coding of sky polarization in insects. *Philos. Trans. R. Soc. Lond. B. Biol. Sci.* 366, 680–7.
464 doi:10.1098/rstb.2010.0199.
465 Huber, R., Hill, S. L., Holladay, C., Biesiadecki, M., Tononi, G., and Cirelli, C. (2004). Sleep
466 homeostasis in Drosophila melanogaster. *Sleep* 27, 628–39. doi:10.1093/sleep/27.4.628.
467 Jenett, A., Rubin, G. M., Ngo, T.-T. B., Shepherd, D., Murphy, C., Dionne, H., et al. (2012). A
468 GAL4-Driver Line Resource for Drosophila Neurobiology. *Cell Rep.* 2, 991–1001.
469 doi:10.1016/j.celrep.2012.09.011.
470 Joiner, W. J., Crocker, A., White, B. H., and Sehgal, A. (2006). Sleep in Drosophila is regulated
471 by adult mushroom bodies. *Nature* 441, 757–760. doi:10.1038/nature04811.
472 Kayser, M. S., Mainwaring, B., Yue, Z., and Sehgal, A. (2015). Sleep deprivation suppresses
473 aggression in Drosophila. *Elife* 4. doi:10.7554/eLife.07643.
474 Kume, K., Kume, S., Park, S. K., Hirsh, J., and Jackson, F. R. (2005). Dopamine is a regulator

475 of arousal in the fruit fly. *J. Neurosci.* 25, 7377–84. doi:10.1523/JNEUROSCI.2048-
476 05.2005.
477 Lamaze, A., Krätschmer, P., Chen, K.-F., Lowe, S., and Jepson, J. E. C. (2018). A Wake-
478 Promoting Circadian Output Circuit in Drosophila. *Curr. Biol.* 28, 3098-3105.e3.
479 doi:10.1016/j.cub.2018.07.024.
480 Lin, C.-Y., Chuang, C.-C., Hua, T.-E., Chen, C.-C., Dickson, B. J., Greenspan, R. J., et al.
481 (2013). A comprehensive wiring diagram of the protocerebral bridge for visual
482 information processing in the Drosophila brain. *Cell Rep.* 3, 1739–53.
483 doi:10.1016/j.celrep.2013.04.022.
484 Liu, Q., Liu, S., Kodama, L., Driscoll, M. R., and Wu, M. N. (2012). Two dopaminergic
485 neurons signal to the dorsal fan-shaped body to promote wakefulness in Drosophila. *Curr.*
486 *Biol.* 22, 2114–23. doi:10.1016/j.cub.2012.09.008.
487 Liu, S., Liu, Q., Tabuchi, M., and Wu, M. N. (2016). Sleep Drive Is Encoded by Neural Plastic
488 Changes in a Dedicated Circuit. *Cell* 165, 1347–1360. doi:10.1016/j.cell.2016.04.013.
489 Martin, J. R., Raabe, T., and Heisenberg, M. (1999). Central complex substructures are required
490 for the maintenance of locomotor activity in Drosophila melanogaster. *J. Comp. Physiol.*
491 *A.* 185, 277–88. doi:10.1007/s003590050387.
492 Nässel, D. R., and Elekes, K. (1992). Aminergic neurons in the brain of blowflies and
493 Drosophila: dopamine- and tyrosine hydroxylase-immunoreactive neurons and their
494 relationship with putative histaminergic neurons. *Cell Tissue Res.*
495 doi:10.1007/BF00318701.
496 Ni, J. D., Gurav, A. S., Liu, W., Ogunmowo, T. H., Hackbart, H., Elsheikh, A., et al. (2019).
497 Differential regulation of the Drosophila sleep homeostat by circadian and arousal inputs.
498 *Elife* 8. doi:10.7554/eLife.40487.
499 Pimentel, D., Donlea, J. M., Talbot, C. B., Song, S. M., Thurston, A. J. F., and Miesenböck, G.
500 (2016). Operation of a homeostatic sleep switch. *Nature* 536, 333–337.
501 doi:10.1038/nature19055.
502 Pitman, J. L., McGill, J. J., Keegan, K. P., and Allada, R. (2006). A dynamic role for the
503 mushroom bodies in promoting sleep in Drosophila. *Nature* 441, 753–756.
504 doi:10.1038/nature04739.
505 Ren, G. R., Folke, J., Hauser, F., Li, S., and Grimmelikhuijzen, C. J. P. (2015). The A- and B-
506 type muscarinic acetylcholine receptors from Drosophila melanogaster couple to different

507 second messenger pathways. *Biochem. Biophys. Res. Commun.* 462, 358–64.
508 doi:10.1016/j.bbrc.2015.04.141.
509 Sbalzarini, I. F., and Koumoutsakos, P. (2005). Feature point tracking and trajectory analysis for
510 video imaging in cell biology. *J. Struct. Biol.* 151, 182–95. doi:10.1016/j.jsb.2005.06.002.
511 Shaw, P. J., Cirelli, C., Greenspan, R. J., and Tononi, G. (2000). Correlates of sleep and waking
512 in Drosophila melanogaster. *Science* 287, 1834–7. doi:10.1126/science.287.5459.1834.
513 Shearin, H. K., Quinn, C. D., Mackin, R. D., Macdonald, I. S., and Stowers, R. S. (2018). t-
514 GRASP, a targeted GRASP for assessing neuronal connectivity. *J. Neurosci. Methods* 306,
515 94–102. doi:10.1016/j.jneumeth.2018.05.014.
516 Sitaraman, D., Aso, Y., Jin, X., Chen, N., Felix, M., Rubin, G. M., et al. (2015a). Propagation of
517 Homeostatic Sleep Signals by Segregated Synaptic Microcircuits of the Drosophila
518 Mushroom Body. *Curr. Biol.* 25, 2915–27. doi:10.1016/j.cub.2015.09.017.
519 Sitaraman, D., Aso, Y., Rubin, G. M., and Nitabach, M. N. (2015b). Control of Sleep by
520 Dopaminergic Inputs to the Drosophila Mushroom Body. *Front. Neural Circuits* 9, 73.
521 doi:10.3389/fncir.2015.00073.
522 Strauss, R., Hanesch, U., Kinkelin, M., Wolf, R., and Heisenberg, M. (1992). No-bridge of
523 Drosophila melanogaster: portrait of a structural brain mutant of the central complex. *J.*
524 *Neurogenet.* 8, 125–55. doi:10.3109/01677069209083444.
525 Strauss, R., and Heisenberg, M. (1993). A higher control center of locomotor behavior in the
526 Drosophila brain. *J. Neurosci.* 13, 1852–61. Available at:
527 http://www.ncbi.nlm.nih.gov/pubmed/8478679 [Accessed January 31, 2020].
528 Triphan, T., Poeck, B., Neuser, K., and Strauss, R. (2010). Visual targeting of motor actions in
529 climbing Drosophila. *Curr. Biol.* 20, 663–8. doi:10.1016/j.cub.2010.02.055.
530 Ueno, T., Tomita, J., Tanimoto, H., Endo, K., Ito, K., Kume, S., et al. (2012). Identification of a
531 dopamine pathway that regulates sleep and arousal in Drosophila. *Nat. Neurosci.* 15,
532 1516–1523. Available at: http://www.nature.com/doifinder/10.1038/nn.3238.
533 Wolff, T., Iyer, N. A., and Rubin, G. M. (2015). Neuroarchitecture and neuroanatomy of the
534 Drosophila central complex: A GAL4-based dissection of protocerebral bridge neurons
535 and circuits. *J. Comp. Neurol.* doi:10.1002/cne.23705.
536 Wu, J. S., and Luo, L. (2006). A protocol for dissecting Drosophila melanogaster brains for live
537 imaging or immunostaining. *Nat. Protoc.* 1, 2110–2115. doi:10.1038/nprot.2006.336.
538

539 **Figure legends**

540

541 **Figure 1.** The PB defective *nob*^{KS49} decreased sleep. Total daily activity **(A)**, total sleep **(B)**
542 and waking activity index **(C)** for control flies (Canton-S, *y w* and *w*^{1118}, white bars) and mutant
543 strains with structural defects in the central complex (black bars) in constant dark (DD) conditions.
544 Data are averaged for 3 days and are presented as mean ± standard error of the mean (SEM) (n =
545 3-11 for each group). Groups with asterisks indicate statistically significant differences (Tukey-
546 Kramer HSD test for normally distributed data, $p < 0.05$).

547

548 **Figure 2.** Acute activation of the PB neurons affected sleep. **(A)** The amount of sleep per day
549 at 29ºC in DD conditions in control flies (black bars) and flies expressing *dTrpA1* transgene by
550 indicated *Gal4* drivers that highly express in PB neurons (red bars). For controls, each *Gal4*
551 driver was crossed with *w*^{1118} (the genetic background of *UAS-dTrpA1* carrying flies). Data are
552 presented as mean ± SEM (n = 6-16 for each group). Asterisks indicate statistically significant
553 differences from control determined by a t-test ($p < 0.05$). **(B)** Sleep profiles for 60-min intervals
554 for controls (*R52B10-Gal4* × *w*^{1118}, black circles, n = 16) or flies expressing *dTrpA1* with *R52B10-*
555 *Gal4* (*R52B10-Gal4* × *UAS-dTrpA1*, red circles, n = 16) in DD. Behavior was monitored in DD
556 for 1 day at 22ºC, followed by 1 day at 29ºC (dTrpA1 activation), and 2 days at 22ºC. Gray and
557 black bars under the horizontal axis indicate subjective day and night, respectively. Data are
558 presented as mean ± SEM. **(C)** Sleep profiles for 60-min intervals for controls (*R59E08-Gal4*
559 × *w*^{1118}, black circles, n = 16) or flies expressing *dTrpA1* with *R59E08-Gal4* (*R59E08-Gal4* ×
560 *UAS-dTrpA1*, blue circles, n = 11) in DD. Mean ± SEM is shown. **(D,E)** Maximum-intensity
561 projection of the confocal brain images of *R52B10-Gal4* **(D)** or *R59E08-Gal4* **(E)** crossed to *UAS-*
562 *mCD8::GFP* flies.

563

564 **Figure supplement 1.** Neuronal activation using *Gal4* drivers that express in the AVLP did not
565 remarkably decrease sleep. **(A)** Sleep profiles for 60-min intervals for controls (*R52H12-Gal4*
566 × *w*^{1118}, black circles, n = 16) or flies expressing *dTrpA1* with *R52H12-Gal4* (*R52H12-Gal4* ×
567 *UAS-dTrpA1*, red circles, n = 16) in DD. The behavior was monitored as described in Figure 2.
568 Mean ± SEM is shown. **(B)** Sleep profiles for 60-min intervals for controls (*R83A10-Gal4* ×
569 *w*^{1118}, black circles, n = 16) or flies expressing *dTrpA1* with *R83A10-Gal4* (*R83A10-Gal4* × *UAS-*
570 *dTrpA1*, red circles, n = 11) in DD.

571

572 **Figure supplement 2.** Neuronal activation using *Gal4* drivers that express in the medulla cells
573 did not increase sleep. **(A)** Sleep profiles for 60-min intervals for controls (*R14F09-Gal4* × w^{1118},
574 black circles, n = 16) or flies expressing *dTrpA1* with *R14F09-Gal4* (*R14F09-Gal4* × *UAS-*
575 *dTrpA1*, red circles, n = 16) in DD. The behavior was monitored as described in Figure 2.
576 Mean ± SEM is shown. **(B)** Sleep profiles for 60-min intervals for controls (*R59A12-Gal4* ×
577 w^{1118}, black circles, n = 15) or flies expressing *dTrpA1* with *R59A12-Gal4* (*R59A12-Gal4* × *UAS-*
578 *dTrpA1*, red circles, n = 16) in DD.

579

580 **Figure 3.** *R59E08-Gal4*-expressing PB interneurons promote sleep. **(A)** Maximum-intensity
581 projection of the confocal brain or ventral nerve cord (VNC) images of flies expressing *UAS-*
582 *mCD8::GFP* under the control of *R59E08-Gal4* (left two panels) or *R59E08-Gal4* with *tsh-Gal80*
583 (right two panels). Transgene *tsh-Gal80* efficiently suppressed *R59E08-Gal4* driven GFP
584 expression in the VNC, while did not in the brains. **(B)** Sleep profiles in 60-min intervals for
585 control flies (*R59E08-Gal4* × *tsh-Gal80*, black circles, n = 12) or flies expressing *dTrpA1* in
586 *R59E08-Gal4* brain neurons (*R59E08-Gal4* × *tsh-Gal80*; *UAS-dTrpA1*, blue circles, n = 11) in
587 DD. The behavior was monitored as described in Figure 2. **(C)** Horizontal movements of the
588 centroid of three representative control flies (*R59E08-Gal4* × *tsh-Gal80*, black circles) or flies
589 expressing *dTrpA1* in *R59E08-Gal4* brain neurons (*R59E08-Gal4* × *tsh-Gal80*; *UAS-dTrpA1*,
590 blue circles) in a glass tube at 29°C during the late subjective day (CT 8 to CT 12). Positions of
591 the cotton plug and the food were at the top and the bottom in each plot, respectively. The
592 behavior of flies was recorded at 2 frames/sec using an infrared video camera in DD conditions.
593 The fly position in a glass tube was calculated as the center of gravity for each image using ImageJ.
594 **(D)** Sleep profiles in 60-min intervals for control flies (*R59E08-Gal4* × w^{1118}, black circles, n =
595 16) or flies expressing *dTrpA1* in *R59E08-Gal4* except cholinergic neurons (*R59E08-Gal4* × *tsh-*
596 *Gal80*; *UAS-dTrpA1*; $Cha^{7.4kb}$*-Gal80*, blue circles, n = 16) in DD.

597

598 **Figure 4.** *R52B10-Gal4*-expressing PFN neurons promote wakefulness. **(A)** Maximum-
599 intensity projection of the confocal brain or VNC images of flies expressing *UAS-mCD8::GFP*
600 under the control of *R52B10-Gal4* (left two panels) or *R52B10-Gal4* with *tsh-Gal80* (right two
601 panels). The *tsh-Gal80* efficiently suppressed *R52B10-Gal4* driven GFP expression in the VNC,
602 while did not in the brains. **(B)** Sleep profiles in 60-min intervals for control flies (*R52B10-*

603 *Gal4* × *tsh-Gal80*, black circles, $n = 16$) or flies expressing *dTrpA1* in *R59E08-Gal4* brain neurons
604 (*R59E08-Gal4* × *tsh-Gal80*; *UAS-dTrpA1*, blue circles, $n = 16$) in DD. The behavior was
605 monitored as described in Figure 2. **(C)** Using the MARCM system, *dTrpA1* expression was
606 targeted to a limited number of neurons in *R52B10-GAL4*. The behavior of mosaic flies was
607 monitored as described in Figure 2. Sleep change (ΔSleep) of a single fly was calculated by
608 subtracting the amount of sleep during the subjective night at 29°C from that at 22°C (before
609 29°C) ($n = 133$). The red horizontal bar indicates the mean. **(D,E)** Maximum-intensity
610 projection of the confocal brain images of the flies whose ΔSleep were > +2 SD higher than the
611 mean (red oval) **(D)** or nearly equal to the mean **(E)**. **(F)** Maximum-intensity projection of the
612 confocal brain images of *c465-Gal4*, *MB247-Gal80* crossed to *UAS-mCD8::GFP* flies. *c465-*
613 *Gal4* drives expression in the PFN neurons. **(G)** Sleep profiles in 60-min intervals for control
614 (*c465-Gal4*, *MB247-Gal80* × w^{1118}, black circles, $n = 15$) or flies expressing *dTrpA1* in *c465-Gal4*
615 except for mushroom body neurons (*c465-Gal4*, *MB247-Gal80* × *UAS-dTrpA1*; *UAS-dTrpA1*, red
616 circles, $n = 11$) in DD conditions. Behavior was monitored as described in Figure 2, except that
617 flies were transferred to 29°C for 2 days to allow dTrpA1 activation.
618
619 **Figure 5.** The sleep-promoting PB interneurons form synaptic contacts with the wake-
620 promoting PFN neurons. **(A)** The dendritic arbors and presynaptic terminals of the PFN neurons
621 in *R52B10-Gal4* were visualized by expression of the postsynaptic marker DenMark and the
622 presynaptic marker syt-GFP, respectively. **(B)** The neuronal connection of the sleep-promoting
623 PB interneurons to the wake-promoting PFN neurons was revealed using the t-GRASP method.
624 The *pre-t-GRASP* and the *post-t-GRASP* encode the split-GFP fragments, which are targeted to
625 presynaptic endings and dendritic terminals, respectively. Brains expressing *pre-t-GRASP* with
626 *R59E08-Gal4* and *post-t-GRASP* with *R52B10-LexA* were stained with a reconstituted GFP-
627 specific antibody.
628
629 **Figure 6.** Dopamine regulates sleep by acting on the sleep-promoting PB interneurons. **(A)**
630 Maximum-intensity projection of the confocal brain images of *TH-Gal4*, FLP^{243} crossed to
631 *UAS>stop>mCD8::GFP* flies. *TH-Gal4*, FLP^{243} restricts expression to the T1 dopaminergic
632 (DA) neurons that project to the PB. **(B)** Sleep profiles in 30-min intervals for control (*TH-Gal4*
633 × *UAS>stop>dTrpA1*, black circles, $n = 15$) or flies expressing *dTrpA1* in T1 DA neurons (*TH-*
634 *Gal4*, FLP^{243} × *UAS>stop>dTrpA1*, red circles, $n = 16$) in DD conditions. The behavior was

635 monitored as described in Figure 2. **(C,D)** The anatomical connection of DA neurons in *TH-*
636 *Gal4* to the sleep-promoting PB interneurons (C) or the wake-promoting PFN neurons (D) were
637 examined using the GRASP method. Brains were stained with a reconstituted GFP-specific
638 antibody. **(E)** Total daily sleep for control (white bar, $n = 15$) and *Dop2R* RNAi-expressing flies
639 using the *R59E08-Gal4* driver (black bars, $n = 16$) in DD conditions. Data are averaged for 3
640 days and are presented as mean ± SEM. $*p < 0.05$; *t*-test.
641
642 **Figure supplement 1.** *Dop2R* knockdown with *R59E08-Gal4* increased sleep. **(A)** Total daily
643 sleep for control (*UAS-Dicer-2*;*R59E08-Gal4* × w^{1118}, white bar, $n = 13$) and *Dop2R* RNAi
644 (VDRC 1820)-expressing flies using the *R59E08-Gal4* driver (black bars, $n = 13$) in DD
645 conditions. Data are averaged for 3 days and are presented as mean ± SEM. $*p < 0.05$; *t*-test.

Figure 1

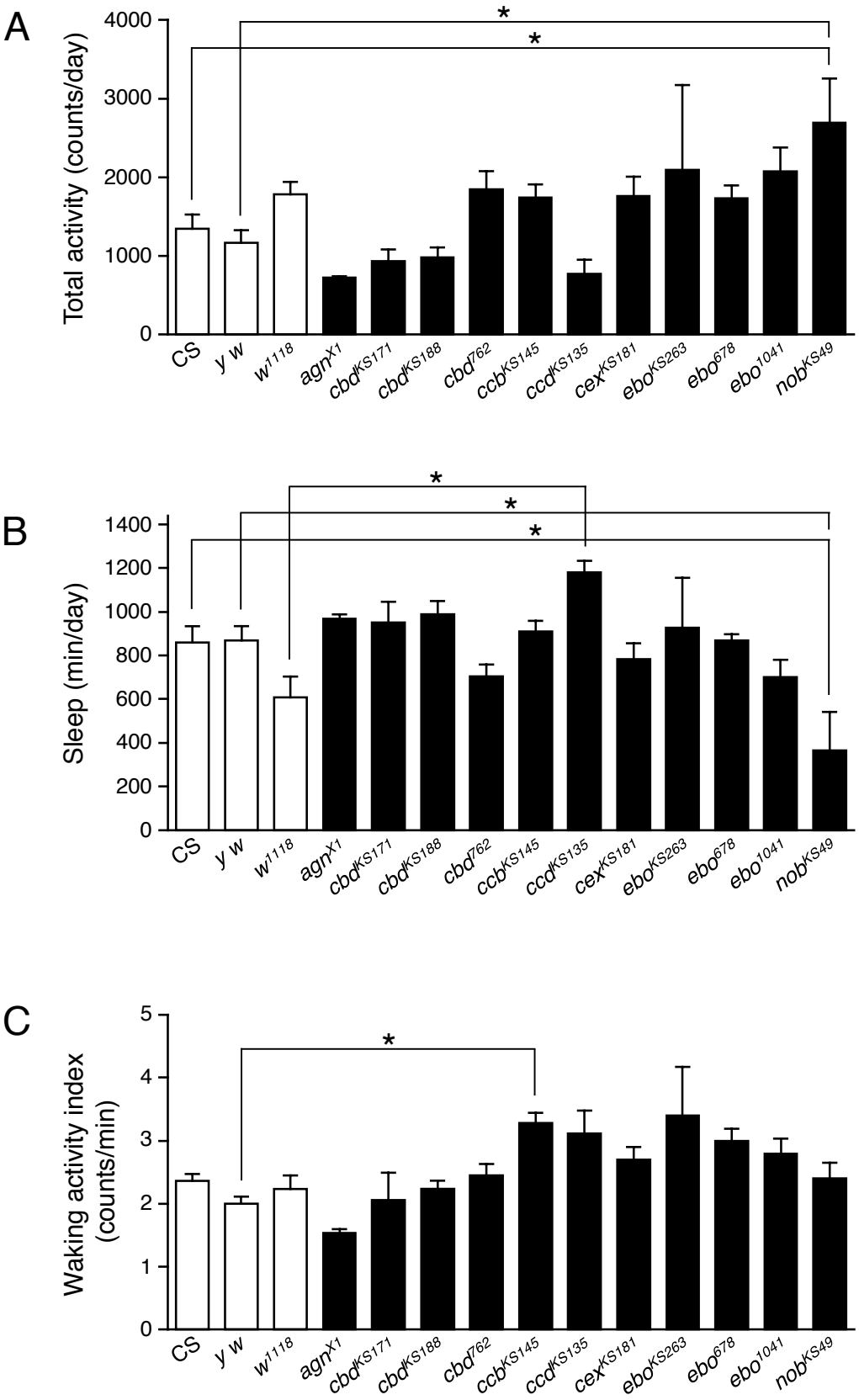
A
Total activity (counts/day)
4000
3000
2000
1000
0
*
*
CS
y w
w1118
agnX1
cbdKS171
cbdKS188
cbd762
ccbKS145
ccdKS135
cexKS181
eboKS263
ebo678
ebo1041
nobKS49
B
Sleep (min/day)
1400
1200
1000
800
600
400
200
0
*
*
*
C
Waking activity index (counts/min)
5
4
3
2
1
0
*

Figure 2

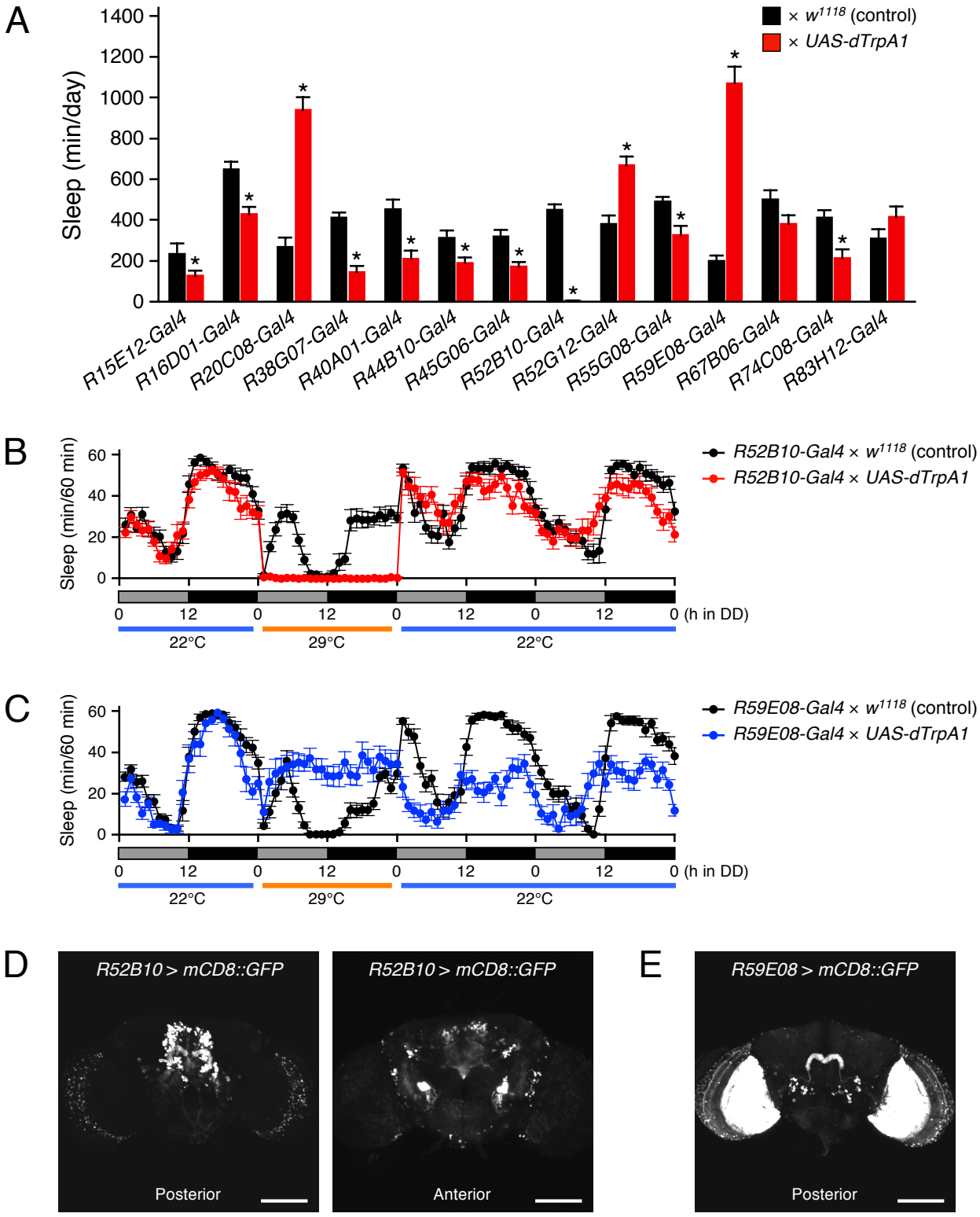
A
Sleep (min/day)
1400
1200
1000
800
600
400
200
0
× w1118 (control)
× UAS-dTrpA1
R15E12-Gal4
R16D01-Gal4
R20C08-Gal4
R38G07-Gal4
R40A01-Gal4
R44B10-Gal4
R45G06-Gal4
R52B10-Gal4
R52G12-Gal4
R55G08-Gal4
R59E08-Gal4
R67B06-Gal4
R74C08-Gal4
R83H12-Gal4
B
Sleep (min/60 min)
R52B10-Gal4 × w1118 (control)
R52B10-Gal4 × UAS-dTrpA1
0 12 0 12 0 12 0 12 0 (h in DD)
22°C
29°C
22°C
C
Sleep (min/60 min)
R59E08-Gal4 × w1118 (control)
R59E08-Gal4 × UAS-dTrpA1
0 12 0 12 0 12 0 12 0 (h in DD)
22°C
29°C
22°C
D
R52B10 > mCD8::GFP
Posterior
R52B10 > mCD8::GFP
Anterior
E
R59E08 > mCD8::GFP
Posterior

Figure 3

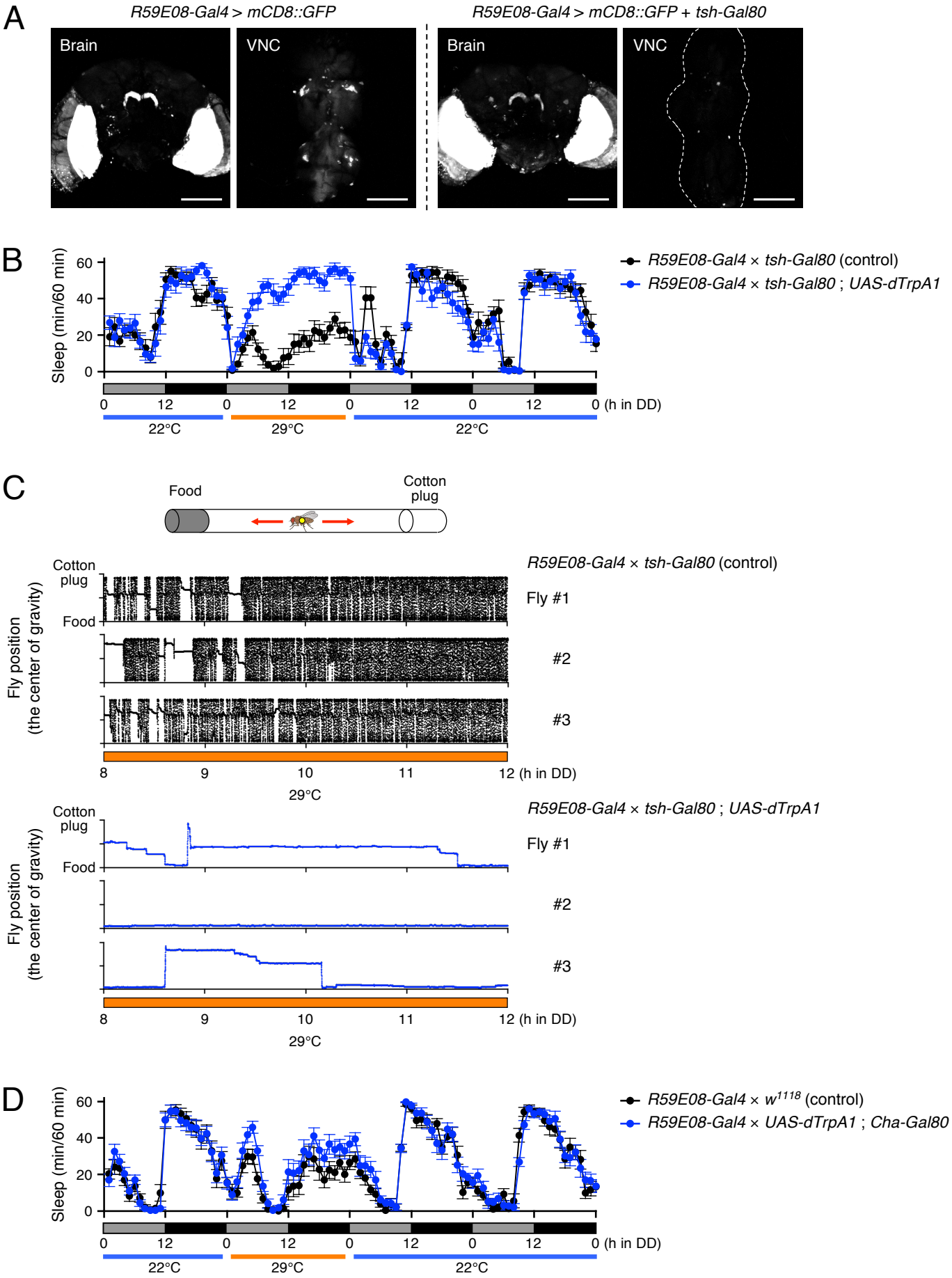
A
R59E08-Gal4 > mCD8::GFP
R59E08-Gal4 > mCD8::GFP + tsh-Gal80
Brain
VNC
Brain
VNC
B
Sleep (min/60 min)
60
40
20
0
0
12
0
12
0
12
0
12
0 (h in DD)
22°C
29°C
22°C
R59E08-Gal4 × tsh-Gal80 (control)
R59E08-Gal4 × tsh-Gal80 ; UAS-dTrpA1
C
Food
Cotton plug
Cotton plug
Food
Fly position (the center of gravity)
R59E08-Gal4 × tsh-Gal80 (control)
Fly #1
#2
#3
8
9
10
11
12 (h in DD)
29°C
Cotton plug
Food
Fly position (the center of gravity)
R59E08-Gal4 × tsh-Gal80 ; UAS-dTrpA1
Fly #1
#2
#3
8
9
10
11
12 (h in DD)
29°C
D
Sleep (min/60 min)
60
40
20
0
0
12
0
12
0
12
0
12
0 (h in DD)
22°C
29°C
22°C
R59E08-Gal4 × w1118 (control)
R59E08-Gal4 × UAS-dTrpA1 ; Cha-Gal80

Figure 4

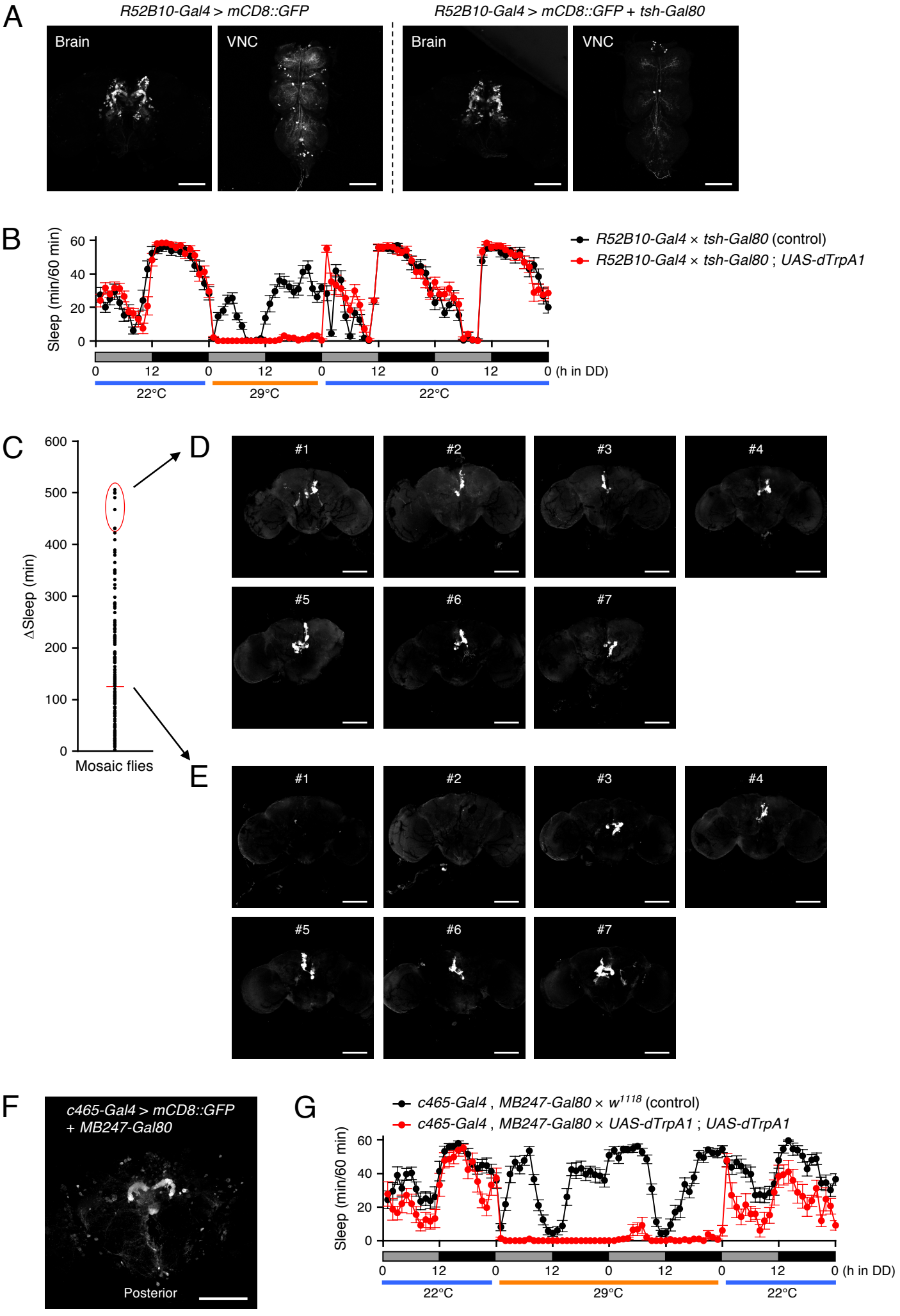
A
R52B10-Gal4 > mCD8::GFP
R52B10-Gal4 > mCD8::GFP + tsh-Gal80
Brain
VNC
Brain
VNC
B
Sleep (min/60 min)
60
40
20
0
R52B10-Gal4 × tsh-Gal80 (control)
R52B10-Gal4 × tsh-Gal80 ; UAS-dTrpA1
0
12
0
12
0
12
0
12
0 (h in DD)
22°C
29°C
22°C
C
ΔSleep (min)
600
500
400
300
200
100
0
Mosaic flies
D
#1
#2
#3
#4
#5
#6
#7
E
#1
#2
#3
#4
#5
#6
#7
F
c465-Gal4 > mCD8::GFP
+ MB247-Gal80
Posterior
G
c465-Gal4 , MB247-Gal80 × w1118 (control)
c465-Gal4 , MB247-Gal80 × UAS-dTrpA1 ; UAS-dTrpA1
Sleep (min/60 min)
60
40
20
0
0
12
0
12
0
12
0
12
0 (h in DD)
22°C
29°C
22°C

Figure 5

A

R52B10-Gal4 > DenMark, syt-GFP

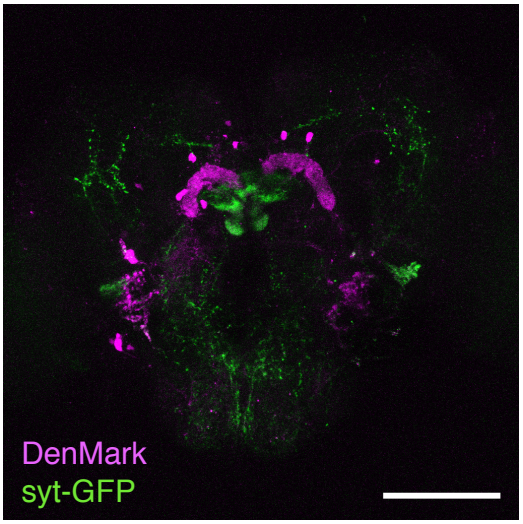

B

R59E08-Gal4 > pre-t-GRASP
R52B10-LexA > post-t-GRASP

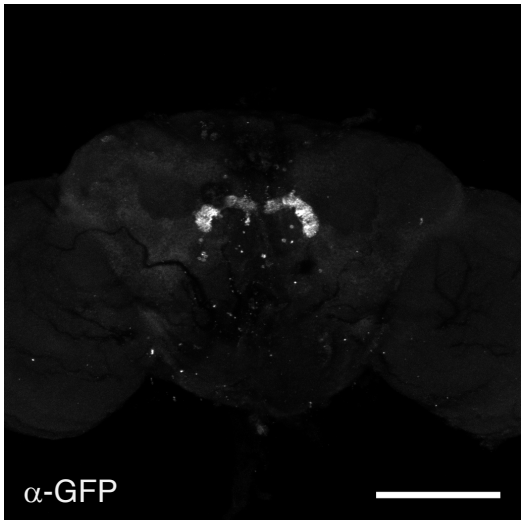

Figure 6

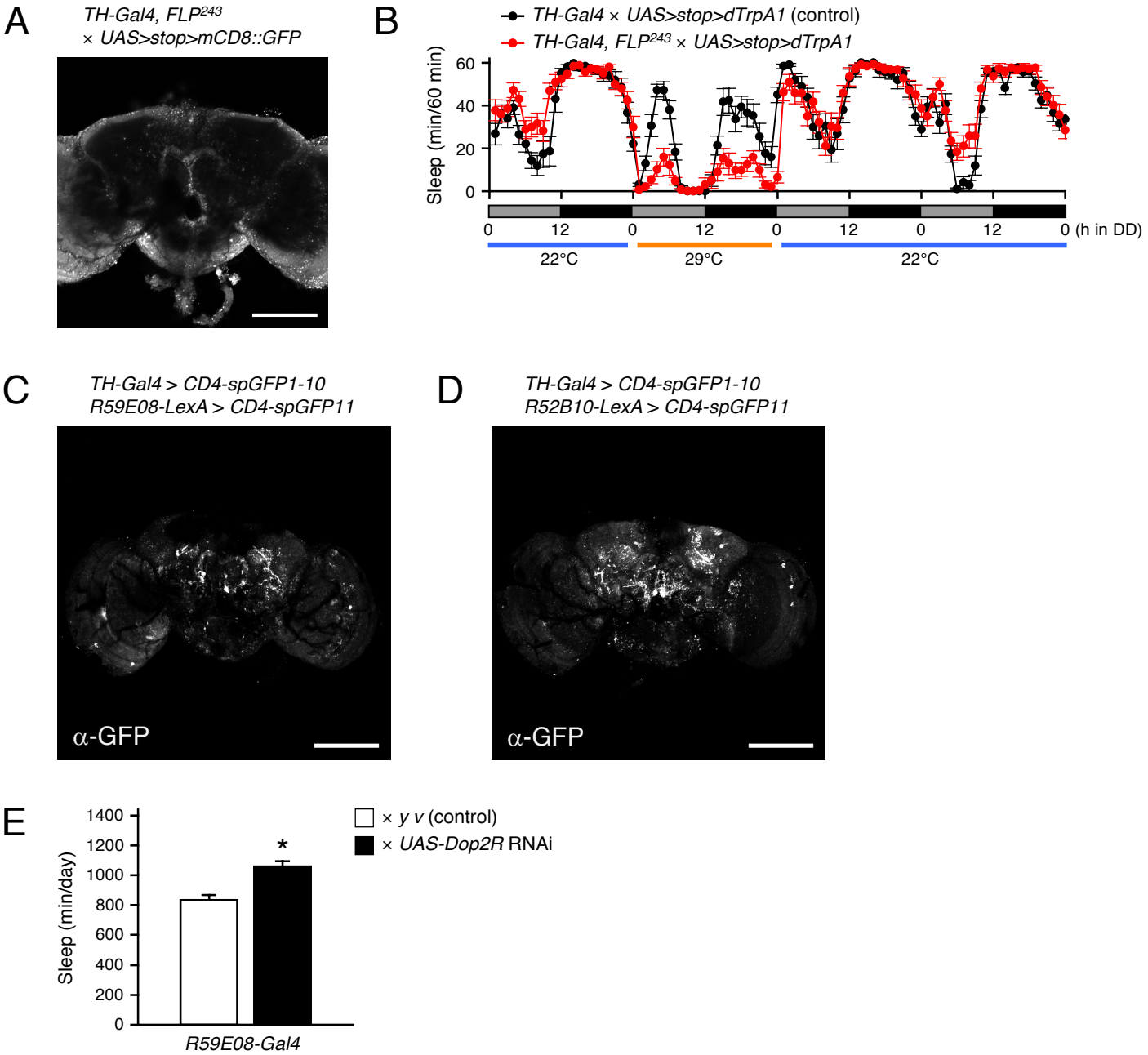
A
TH-Gal4, FLP243
× UAS>stop>mCD8::GFP
B
TH-Gal4 × UAS>stop>dTrpA1 (control)
TH-Gal4, FLP243 × UAS>stop>dTrpA1
Sleep (min/60 min)
60
40
20
0
0
12
0
12
0
12
0
12
0 (h in DD)
22°C
29°C
22°C
C
TH-Gal4 > CD4-spGFP1-10
R59E08-LexA > CD4-spGFP11
α-GFP
D
TH-Gal4 > CD4-spGFP1-10
R52B10-LexA > CD4-spGFP11
α-GFP
E
Sleep (min/day)
1400
1200
1000
800
600
400
200
0
*
× y v (control)
× UAS-Dop2R RNAi
R59E08-Gal4